Oxidation of photochromic spirooxazines by coinage metal cations.

Part II. Oxidation by gold(III) compounds and synthesis of gold colloids†

Pawel Uznanski,*[a] Catherine Amiens,[b] Manuel Bardaji,[c] Bruno Donnadieu,[b] Yannick Coppel,[b] Bruno Chaudret[b] and Antonio Laguna[c]

[a] *Centre for Molecular and Macromolecular Studies, Polish Academy of Sciences, Sienkiewicza 112, 90-363, Lodz, Poland. E-mail: puznansk@bilbo.cbmm.lodz.pl*

[b] *Laboratoire de Chimie de Coordination, CNRS, 205 Route de Narbonne, F-31077 Toulouse cedex 4, France. E-mail: chaudret@lcc-toulouse.fr, amiens@lcc-toulouse.fr*

[c] *Departamento de Quimica Inorganica, Instituto de Ciencia de Materiales de Aragon, Universidad de Zaragoza-CSIC, E-50009, Zaragoza, Spain*

Received (in Montpellier, France) 18th June 2001, Accepted 12th September 2001
First published as an Advance Article on the web

In our previous paper, we reported that colloidal silver can be prepared by thermal or photo-oxidation processes of spirooxazines (SO). Here we show that SO easily reduce gold(III) ions (1 : 1 equiv.) to monovalent gold(I) species. A salt composed of oxidized dye/Au^{I} was isolated and fully characterised by X-ray diffraction, ^{1}H and ^{13}C NMR, UV-vis, fluorescence and FTIR spectroscopies. This salt was further reduced by another SO (2 : 1 equiv.) leading to gold(0) atoms that coalesce into gold powder. A mechanism for these two reactions is proposed. In the presence of a stabilising agent, such as poly(*N*-vinylpyrrolidone), the coalescence of Au atoms is limited and nanoparticles with an average size of 8–14 nm and a broad size distribution are formed. The colloidal solution is strongly fluorescent due to the presence of the oxidized SO in the medium. Changes in the absorption spectra from that of the sol and the free oxidized SO are interpreted as a consequence of the adsorption of the cationic dye on the gold surface.

Considerable research has focused on the synthesis, physical and photochemical properties of photochromic spiropyrans (SP) and spirooxazines (SO).[1,2] These compounds show thermally reversible changes of structure and colour upon light irradiation, thus attracting interest due to their potential use, as components of light protective materials, in optical switches and devices, recording media, *etc*. Their photochromic properties are due to the C_{spiro}–O bond cleavage induced by ultraviolet irradiation or heating, followed by the formation of a polar, metastable merocyanine (Mc) entity (Scheme 1). Unfortunately, the limited stability of the photochromic spiro compounds when dispersed in various media and after exposure to light,[3–5] strongly reduces their utility in common applications. One of the mechanisms recently reported for the degradation of the photochromic dyes involves oxidation processes.[6,7] There have been recent reports concerning the identification of the degradation product and several mechanisms of degradation have been proposed.[8] For instance, the Mc form was shown to be reactive towards trimethylsilyl cyanide or free radicals and give zwitterionic adducts.[9,10]

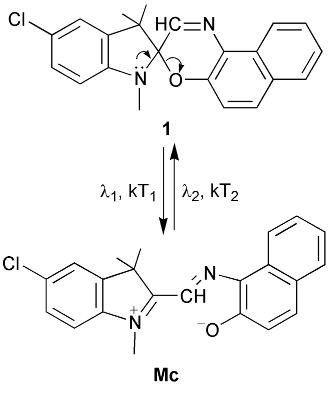

Scheme 1

In a previous paper we have shown that the oxidative chemistry of spirooxazines with monovalent silver ions in alcohols is surprisingly rich, yielding non-photochromic alkoxy derivatives of the parent spiro compounds and rearranged indolinonaphthoxazole products. These products are further hydrolysed to a neutral (hydroxyindolino) naphthoxazole displaying a characteristic blue emission.[11] We have proposed a mechanism that clarifies the thermal reaction channel for the oxidation of SO. Although products involved in redox processes were characterised by ^{1}H and ^{13}C NMR, and some of them by X-ray diffraction analysis, we were not able to isolate single crystals of the major product, namely an oxazole salt. However, it would be interesting to compare the crystal structure of such organic/inorganic salts with previously reported crystal data for a similar but fully organic system. To simplify the reaction we chose trivalent metal ions instead of monovalent silver; this should promote a transfer of two electrons to only one electron acceptor species. In order to achieve an efficient oxidative reaction that would meet our expectations, we turned our attention to photochromic 5-chloro-1,3-dihydro-1,3,3-trimethylspiro(2*H*-indole-2,3′-[3*H*]naphth[2,1-*b*]-[1,4]oxazine) (**1**) and to a tetrachloroaurate(III) salt. Such compounds crystallise easily and are more resistant to degradation[6,11] while the presence of gold atoms may, accordingly, lead to the formation of a colloid. Furthermore,

---

† For part 1, see ref. 11.

DOI: 10.1039/b105447n

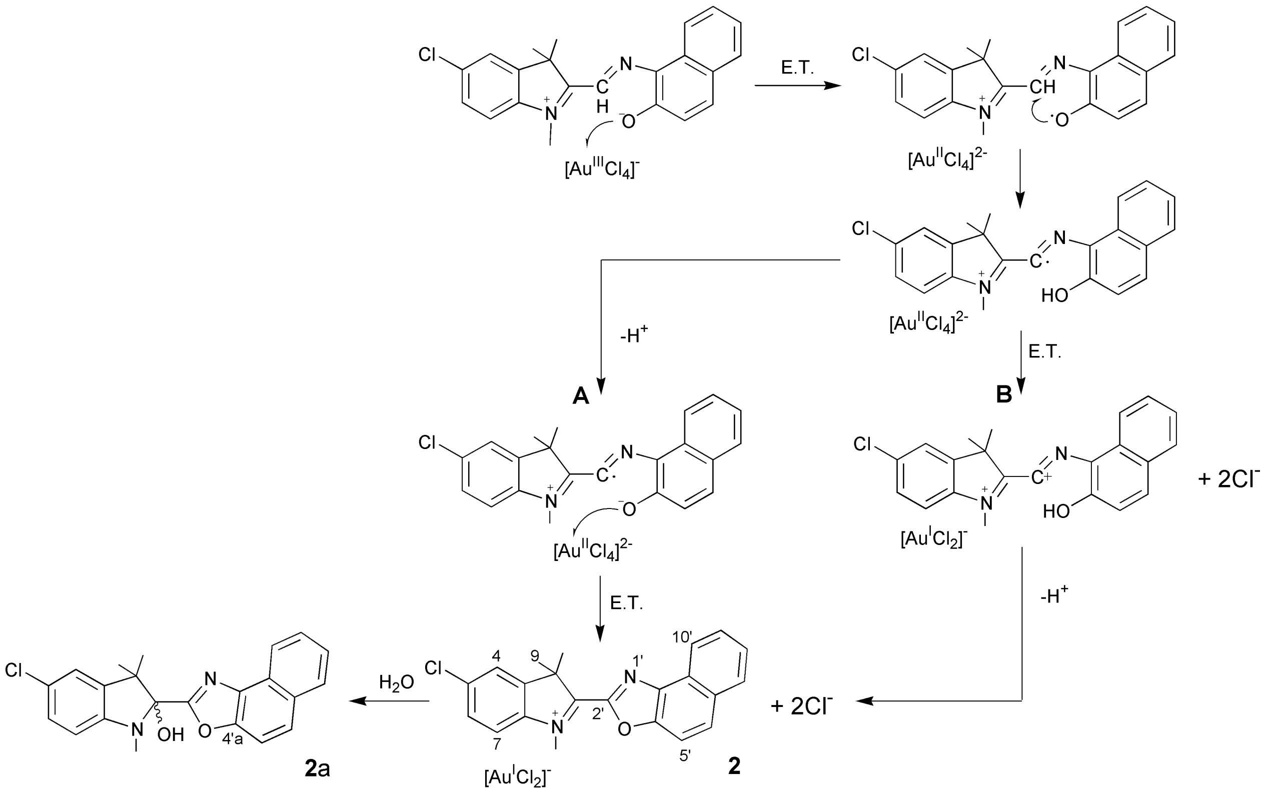

Scheme 2

as the two main oxidation states of gold are Au$^{\mathrm{III}}$ and Au$^{\mathrm{I}}$, the use of $\mathrm{AuCl_4}^-$ was supposed to promote a 1 : 1 reaction with the SO. Indeed, the reduction of Au$^{\mathrm{III}}$ to Au$^{\mathrm{I}}$ turns out to be fast but the next reduction step is much slower, which allowed us to isolate the intermediate Au$^{\mathrm{I}}$ salt as a crystalline compound and characterise it by an X-ray diffraction study. The gold nanoparticles formed at the end of the reaction have been fully analysed by TEM (transmission electron microscopy) and UV-vis absorption spectroscopy. Finally, we propose a mechanism for the redox reactions and compare it with that already reported for Ag$^{\mathrm{I}}$ reduction by analogous spirooxazine compounds.

Results and discussion

Thermal oxidation of 1

Addition of sodium tetrachloroaurate to an acetonitrile solution of **1** leads within a few minutes to a colour change from colourless to orange. The colour is associated with an electronic absorption band with a maximum at 465 nm, corresponding to a new compound. This indicates that the π-electron systems of two reciprocally perpendicular parts of the parent molecule start interacting strongly due to their coplanarity. However, the band cannot be attributed to the open Mc form, the absorbance of which would be expected at ~600 nm. ^{1}H NMR analysis of the solution also supports the presence of a new species **2** in the mixture. It shows two singlets at 7.74 and 2.74 ppm, corresponding respectively to protons at –CH=N– and N–CH$_3$ characteristic for spirooxazine ring opening. The former resonance finally disappears from the spectrum whereas the latter shifts its position to 4.70 ppm, characteristic of the quaternary nitrogen. Reaction of **1** with Cl$_4$AuNa in refluxing acetonitrile under argon for 1.5 h yields a rearranged product **2** and NaCl crystals. Analytically pure samples of **2**·$[\mathrm{AuCl_2}]^-$ were crystallised from a mixture of acetonitrile and methanol (3 : 1) at 4 °C. Product structures were assigned on the basis of ^{1}H and ^{13}C NMR and X-ray diffraction data.

Thermal oxidation of **1** is likely to proceed according to the mechanism described before,[11] which includes two complementary reaction paths (Scheme 2). A first electron transfer occurs from the oxygen atom to the Au$^{\mathrm{III}}$ ion. A more stable radical forms by 1,5-hydrogen transfer from C2′. Then two paths can be envisaged, whether the second electron transfer occurs prior to a deprotonation step (route B) or after it (route A).

The conversion of $[\mathrm{Au^{III}Cl_4}]^-$ ion to $[\mathrm{Au^{I}Cl_2}]^-$ with elimination of chloro ligands is supposed to proceed through transient formation of the $[\mathrm{Au^{II}Cl_4}]^{2-}$ ion.[12] In the presence of water **2** is hydrolysed to (hydroxyindolino)naphthoxazole (**2a**).[6]

Salt **2**·$[\mathrm{AuCl_2}]^-$ can be further reduced by **1** (Scheme 3) into the chloride salt of **2**. As the oxidative degradation of spirooxazines involves transfer of two electrons from the open zwitterionic Mc form to the appropriate electron acceptor molecule, two gold(I) ions are reduced by one spirooxazine molecule. As a result of the coalescence of the resulting elemental gold atoms, gold powder precipitates from the reaction solution.

X-Ray crystallographic results for 2 as the $[\mathrm{AuCl_2}]^-$ salt

Salt **2**·$[\mathrm{AuCl_2}]^-$ has been analysed by a single-crystal X-ray study, the results of which are presented in Table 1 and shown in Fig. 1. The solid state structure of **2** is similar to that of the other oxazole salt characterized by X-ray crystallography.[7] The compound is planar with the indoline part linked through a C–C bridge to the naphthoxazole ring. The unit cell consists of two asymmetric units with two sets of **2**·$[\mathrm{AuCl_2}]^-$ pairs, respectively A and B. In each unit the **2** cations are stacked and twisted so that their indoline heterocycles overlap with a distance of 7.662(2) Å between the N(2A) and N(2B) atoms. In turn the dyes from the two different units B and B′ are arranged in a fishbone-like pattern. The distances between gold atoms and charged nitrogen atoms are 5.529(1) and 4.107(2) Å, in pairs A and

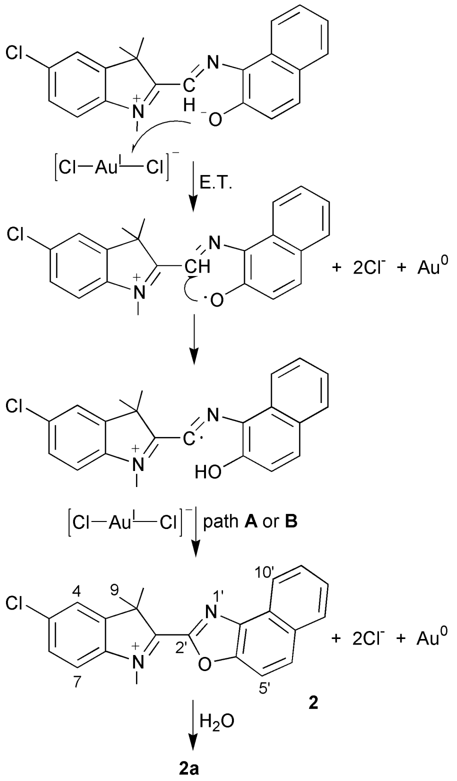

Scheme 3

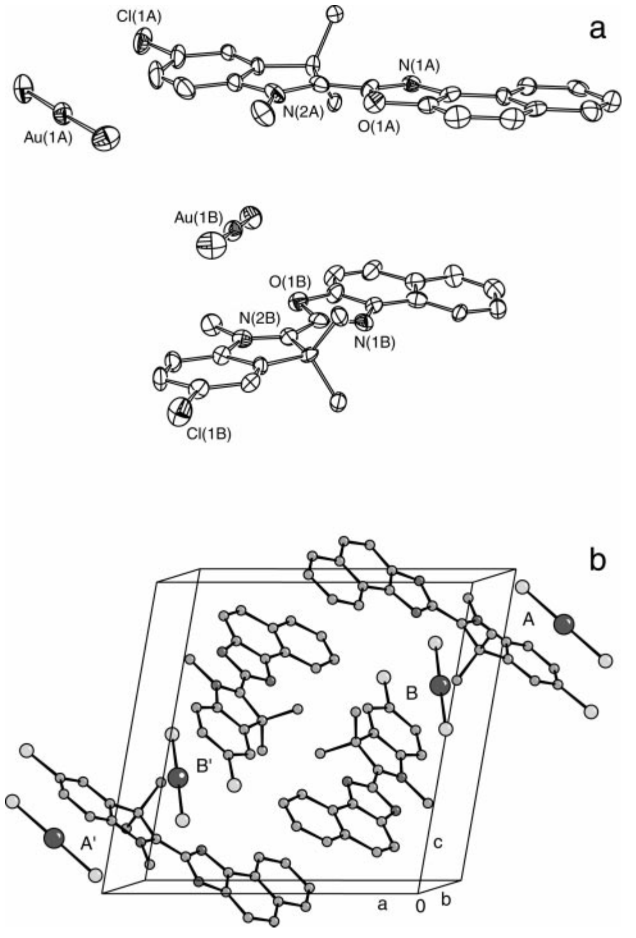

Fig. 1 (a) The structure and atomic numbering of **2**·[AuCl$_2$]$^-$ with thermal ellipsoids drawn at the 40% probability level. Selected bond lengths (Å) and angles (°) are as follows: Au(1B)–Cl(3B), 2.248(3); Au(1B)–Cl(2B), 2.256(3); Cl(1B)–C(16B), 1.740(9); O(1B)–C(1B), 1.379(1); N(1B)–C(1B), 1.281(13); N(2B)–C(22B), 1.479(1); C(1B)–C(12B), 1.478(1); C(12B)–C(19B), 1.504(1). Cl(3B)–Au(1B)–Cl(2B), 178.42(1); C(12B)–N(2B)–C(22B), 128.3(9); N(1B)–C(1B)–O(1B), 117.5(10); N(1B)–C(1B)–C(12B), 123.4(1); N(2B)–C(12B)–C(1B), 124.8(9); N(2B)–C(12B)–C(19B), 112.7(9); C(21B)–C(19B)–C(20B), 110.8(8). (b) Unit cell of **2**·[AuCl$_2$]$^-$. Selected intermolecular distances (Å): Au(1A)···N(2A), 5.529(1); Au(1B)···N(2B), 4.107(2); Au(1B)···N(2A), 3.879(1); Au(1A)···N(2B), 8.952(2); Au(1A)···Au(1B), 5.630(1); Au(1B)···Au(1B), 12.572(2); N(2B)···N(2B), 9.198(1); N(2A)···N(2B), 7.662(2); Au(1A)···C(15A), 3.872(1).

B respectively, while gold atoms are separated by 5.630(1) Å. The [AuCl$_2$]$^-$ anion from the B couple is located between two dyes and the distance Au(1B)–N(2A) equals 3.879(1) Å. Thus, it is shorter than the distance Au(1B)–N(2B), suggesting that the negative charge on [AuCl$_2$]$^-$ is shared between the two cations. The [AuCl$_2$]$^-$ anion in A is coplanar with **2** and the Au(1A) gold atom is separated from the positive charge on N(2B) by as much as 8.952(2) Å. The packing of the **2**·[AuCl$_2$]$^-$ crystal provides experimental evidence for its non-conductive properties. The crystal structure contrasts with that recently reported by Malatesta *et al.*: the organic TCNQ$_2^{\bullet-}$ ion radical salt of an oxazole, in which anions and cations form segregated stacks.[7] In this case, electron delocalisation on helically arranged TCNQ pairs is in agreement with both a low resistivity for the microcrystals and paramagnetic character. Selected bond lengths and angles for the **2**·[AuCl$_2$]$^-$ salt are given in Fig. 1. The crystals were not stable and turned to powder within a few weeks, probably due to their sensitivity to water.

Table 1 Crystallographic data for **2**·[Cl$_2$Au]$^-$

Formula	$C_{22}H_{18}NOCl_3Au$
FW	629.70
Crystal system	Triclinic
Space group	$P\bar{1}$
a/Å	12.5891(2)
b/Å	13.6746(2)
c/Å	14.2577(2)
α/°	114.178(1)
β/°	97.965(2)
γ/°	98.965(1)
U/Å^3	2155.3(5)
Z	4
T/K	180
Reflections collected	15984
Unique reflections	5839
R_{int}	0.0720
R	0.0364
wR	0.0650

Electronic and luminescence spectra

In agreement with our previous studies on oxidation products of the photochromic spirooxazines,[11] the salt prepared in this study has similar absorption spectra with a broad and intense transition between 400–500 nm (the chlorine substituent has little effect on the photophysical properties). The excited state is strongly fluorescent ($\Phi_f > 0.85$ in acetonitrile) with an emission maximum at 535 nm (Fig. 2). This is not surprising, as the fluorescence of oxazoles is known to be strongly enhanced when attached to an aromatic hydrocarbon.[13] The hypsochromic shift of the absorption band and blue fluorescence of **2a** is connected with its non-planar geometry. For both products a large Stokes shift and a high fluorescence quantum yield with fast emission decay are observed.[11]

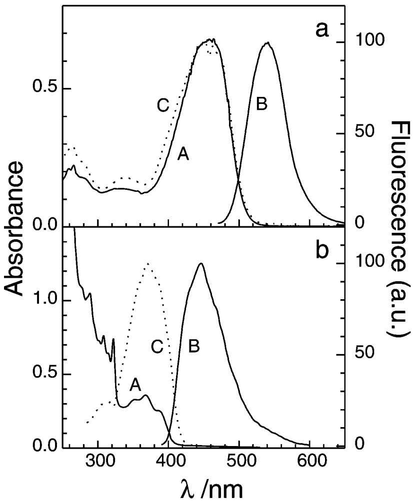

Fig. 2 UV-vis absorption (A), fluorescence excitation (B) and emission (C) spectra. (a) $\mathbf{2}\cdot[AuCl_2]^-$ in acetonitrile. (b) **2a** in EtOH.

Gold nanoparticles

As was mentioned earlier, further reduction of the Au$^{\text{I}}$ anion led to the formation of gold powder. Unfortunately, in the acetonitrile–PVP solution **1** itself undergoes dark degradation processes to products with characteristic strong greenish-orange fluorescence, which are competitive with gold(I) reduction bonds and prevented any clear observation of the gold sol. However, as this effect was not observed for an EtOH–PVP mixture, the reaction was repeated in this medium.

A typical absorption spectrum of the solution, after the reaction of the gold salt $\mathbf{2}\cdot[AuCl_2]^-$ with **1** (2 : 1 equiv.) in the presence of PVP in EtOH is shown in Fig. 3. The orange opalescent colour results from a mixture of two components: a strong absorption by the indolinooxazole cation **2** and the extinction band of colloidal gold. **2** absorbs with a maximum at 462 nm, while the less intense part of the spectrum extending into the red is a signature of gold particles. The absorption due to the nanoparticles was calculated as the difference between the two spectra presented in Fig. 3(a) and its broad maximum falls around 510 nm (inset). This is in good agreement with the characteristic value of 520 nm corresponding to the collective oscillation of free conduction electrons at the surface of spherical gold nanoparticles.[14] The presence of nanoparticles was demonstrated by TEM. In the micrograph of Fig. 3(b) the particles are non-uniform and can be described rather by a bimodal distribution. The sizes of the majority of them are around 14 nm. The second component of the size distribution has an average size of 8 nm [Fig. 3(c)]. Apparently, the particles are not aggregated. We ascribe their alignment on the micrograph to drying effects on the copper grid. The colloidal solution was stable, demonstrating its colour and fluorescence properties for months.

Nucleation and growth of gold clusters is expected to be specific as they are generated by the reduction of $[AuCl_2]^-$ ions by an electron transfer reaction from the Mc entity, which is oxidised to a positively charged species. Indeed, the absorption by **2** is slightly larger than in neat EtOH (458 nm) and the plasmon band is blue shifted, which may suggest that the dye is chemisorbed on the gold particle surfaces. This point, however, needs elucidation using surface enhancement spectroscopic techniques.[15] Some recent results on the adsorption of cationic dyes on gold or silver[11,16] show that dye–metal systems on the nanometric scale are possible.

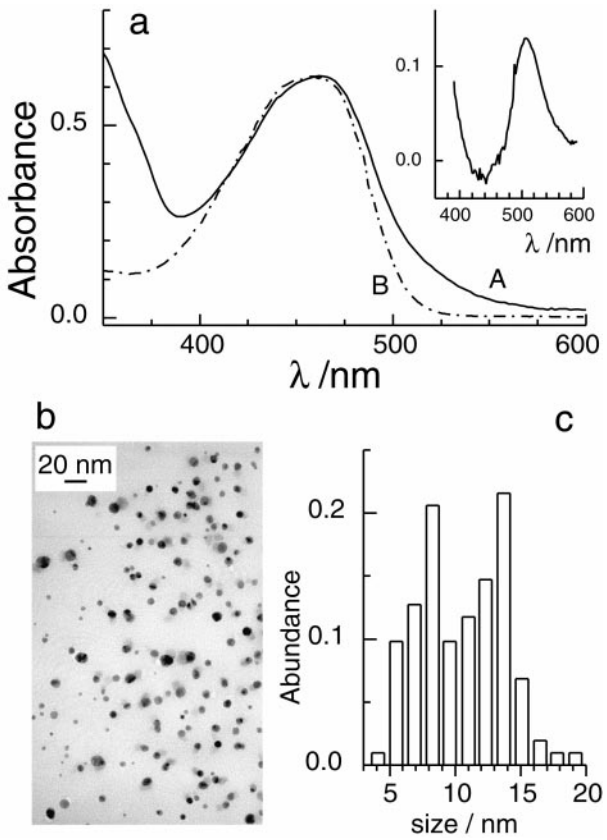

Fig. 3 (a) Extinction spectrum of gold colloid prepared from reduction of Cl_4AuNa by **1** in the presence of PVP in ethanol (A). For comparison the normalised spectrum of **2** in EtOH is also shown (B). Inset. Plasmon spectrum of gold obtained by subtraction of spectrum B from spectrum A. (b) Electron micrograph showing the size of gold particles. The alignment of these particles is due to drying effects on the copper grid. (c) Size distribution of the sample shown in (b).

Conclusions

We have shown that gold(III) salts can be reduced to gold(0) atoms with a stable transient dye/gold(I) salt in a two-step reaction by photochromic spirooxazines. Dispersions of small gold particles were obtained using a stabilising PVP solution. Absorption spectra of the final sol suggest the adsorption of the oxidised spirooxazine on the gold surface. The results may be relevant to various surface enhancement phenomena[15,17] and to the understanding of fundamental processes occurring in photochromic compounds.

The properties of spirooxazines and the strong fluorescence of the oxidative product make it suitable for metal ion sensing, for example. The ability to employ a reversible acid–base reaction to control access to its excited state (Scheme 2) may prove useful in applications using fluorescence methods. Finally we have also found that complex gold precursors, such as ClAuTHT (THT = tetrahydrothiophene), can be reduced by spirooxazines to molecular gold species. The reaction is induced either thermally or by UV irradiation, leading with PVP to formation of gold nanoparticles.

Experimental

Materials

5-Chloro-1,3-dihydro-1,3,3-trimethylspiro(2*H*-indole-2,3′-[3*H*]-naphth[2,1-*b*]-[1,4]oxazine) (**1**) and poly(*N*-vinylpyrrolidone)

(PVP) with an average molecular weight of 4×10^4 were purchased from Aldrich Chemical Co. and used as received. Tetrachloroaurate(III) sodium salt hydrate ($NaCl_4Au \cdot 2H_2O$, analytical reagent) was obtained from Montplet & Esteban (Barcelona, Spain). Acetonitrile was dried over appropriate drying agents and distilled under argon immediately prior to use. All reactions were performed under an atmosphere of argon using standard Schlenk line techniques.

Spectroscopic measurements

UV-visible and infrared absorption spectra were obtained with an HP diode array 8452A spectrophotometer and with an ITI Mattson Infinity FT system. Room-temperature excitation and emission spectra were acquired with a Perkin–Elmer LS50 luminescence spectrometer. The ^{1}H and ^{13}C NMR spectra were recorded at 305 K on a Bruker AMX400 spectrometer operating at 400.13 MHz for ^{1}H and at 100.61 MHz for ^{13}C. All chemical shifts for ^{1}H and ^{13}C were related to TMS using ^{1}H (residual) or ^{13}C chemical shifts of the solvent as a secondary standard. NMR studies were carried out either by one- or two-dimensional NMR methods. The assignments of the ^{1}H resonances were made by 1D or 2D nuclear Overhauser exchange spectroscopy (NOESY) ($t_m = 600$ ms) and 1D total correlation spectroscopy (TOCSY) ($t_m = 60$ ms), whereas 2D heteronuclear correlation techniques (HMQC, HMBC) were used for the complete ^{13}C chemical shift assignments.

Crystallographic structural determination

The single-crystal X-ray diffraction data were collected at 180 K on a Stoe imaging plate diffraction system (IPDS) diffractometer equipped with an Oxford Cryosystems Cryostream cooler device, using Mo-Kα radiation ($\lambda = 0.71073$ Å, $\mu = 5.69\ \mathrm{cm^{-1}}$). Numerical corrections were applied. The structures were solved by direct methods using SIR92, and refined by least-squares procedures on F^2 with the SHELX97 program. All non-hydrogen atoms were refined with anisotropic displacement coefficients, while H atom positions were calculated on geometrical grounds as idealised contributions.

CCDC reference number 171836. See http://www.rsc.org/suppdata/nj/b1/b105447n/ for crystallographic data in CIF or other electronic format.

Preparation of $2 \cdot [AuCl_2]^-$

A mixture of 7.2 mg (2×10^{-5} mol) **1** and 8.4 mg (2.1×10^{-5} mol) $NaCl_4Au \cdot 2H_2O$ were refluxed in acetonitrile (4 ml) under an argon atmosphere for 2 h. After cooling to room temperature NaCl crystals were separated and to the remaining solution 1 ml of MeOH was added. The crystallization at 4 °C overnight gave dark-orange crystals (DSC: $T_m = 89.5$ °C, $Q = 1.185\ \mathrm{J\,g^{-1}}$). ^{1}H NMR ($CD_3CN$): δ 8.73 (dddd, $^3J_{HH} = 8.1$ Hz, $^4J_{HH} = 1.3$ Hz, $^5J_{HH} = 0.6$ Hz, $^5J_{HH} = 0.6$ Hz; 1H, C10′-H), 8.36 (d, $^3J_{HH} = 9.2$ Hz; 1H, C6′-H), 8.24 (dd, $^3J_{HH} = 8.1$ Hz, $^4J_{HH} = 1.3$ Hz; 1H, C7′-H), 8.05 (d, $^3J_{HH} = 9.2$ Hz; 1H, C5′-H), 7.96 (dd, $^3J_{HH} = 8.8$ Hz, $^5J_{HH} = 0.6$ Hz; 1H, C7-H), 7.95 (dd, $^4J_{HH} = 2.0$ Hz, $^5J_{HH} = 0.6$ Hz; 1H, C4-H), 7.94 (ddd, $^3J_{HH} = 8.1$ Hz, $^3J_{HH} = 7.0$ Hz, $^4J_{HH} = 1.3$ Hz; 1H, C9′-H), 7.84 (ddd, $^3J_{HH} = 8.1$ Hz, $^3J_{HH} = 7.0$ Hz, $^5J_{HH} = 1.3$ Hz; 1H, C8′-H), 7.80 (dd, $^3J_{HH} = 8.8$ Hz, $^4J_{HH} = 2.0$ Hz; 1H, C6-H), 4.70 (s; 3H, N^+–CH_3), 2.04 (s; 6H, *gem*-CH_3). $^{13}C\{^1H\}$ NMR (CD_3CN): δ 170.14 (C2), 55.55 (C3), 145.54 (C4a), 124.36 (C4), 137.64 (C5), 130.52 (C6), 118.31 (C7), 141.70 (C7a), 38.73 (C8), 24.28 (C9), 24.28 (C10), 150.90 (C2′), 150.72 (C4′a), 111.80 (C5′), 134.86 (C6′), 132.47 (C6′a), 130.11 (C7′), 128.40 (C8′), 129.83 (C9′), 122.70 (C10′), 126.62 (C10′a), 138.78 (C11′). IR (thin film on SiO_2 support): 1634, 1599, 1571, 1555, 1523, 1489, 1455, 1443, 1426, 1412, 1367, 1342, 1281, 1243, 1225, 1192, 1153, 1111, 1092, 1061, 1012, 925, 822, 808, 759, 730, 696 $\mathrm{cm^{-1}}$. Anal. calc. for $C_{22}H_{18}N_2OCl_3Au$: C, 41.92; H, 2.86; N, 4.44; found: C, 42.5; H, 2.9; N, 4.3%.

Preparation and characterization of colloidal gold

1 (5.4 mg, 1.5×10^{-5} mol) and PVP (22 mg) were dissolved in ethanol (10 mL) and the solution was de-aerated under vacuum. $NaAuCl_4$ (4 mg, 10^{-5} mol) was added under argon. The solution was stirred under reflux for 1 h. Electron micrographs were taken with a JEOL transmission electron microscope model 200CX. TEM samples were obtained by slow evaporation of one drop of the crude solution on a copper grid coated with amorphous carbon. The particle size distribution was obtained from the sample placed on a copper grid coated with amorphous carbon.

Acknowledgements

This work was completed with the support of the European Associated Laboratory financed by CNRS (France), the Polish Committee for Scientific Research (KBN 7 T08E 018 17 project) and Programme de Recherche Franco-Espagnol 2000 PICASSO (no. 00688XH and HF 1999-0122). We thank V. Colliere for technical assistance with the TEM experiments.

References

1 R. C. Bertelson, in *Organic Photochromic and Thermochromic Compounds*, ed. J. C. Crano and R. J. Guglielmetti, Kluwer Academic/Plenum Publishers, New York, 1999, vol. 1, ch. 1.

2 S. Maeda, in *Organic Photochromic and Thermochromic Compounds*, ed. J. C. Crano and R. J. Guglielmetti, Kluwer Academic/Plenum Publishers, New York, 1999, vol. 1, ch. 2.

3 G. Baillet, G. Giusti and R. Guglielmetti, *J. Photochem. Photobiol. A: Chem.*, 1993, **70**, 157.

4 G. Baillet, G. Giusti and R. Guglielmetti, *Bull. Chem. Soc. Jpn.*, 1995, **68**, 1220.

5 G. Baillet, M. Campredon, R. Guglielmetti, G. Giusti and C. Aubert, *J. Photochem. Photobiol. A: Chem.*, 1994, **83**, 147.

6 V. Malatesta, M. Milosa, R. Millini, L. Lanzini, P. Bortolus and S. Monti, *Mol. Cryst. Liq. Cryst.*, 1994, **246**, 303.

7 V. Malatesta, R. Millini and L. Montanari, *J. Am. Chem. Soc.*, 1995, **117**, 6258.

8 V. Malatesta, in *Organic Photochromic and Thermochromic Compounds*, ed. J. C. Crano and R. J. Guglielmetti, Kluwer Academic/Plenum Publishers, New York, 1999, vol. 2, ch. 2.

9 V. Malatesta, C. Neri, M. L. Wis, L. Montanari and R. Millini, *J. Am. Chem. Soc.*, 1997, **119**, 3451.

10 V. Malatesta, F. Renzi, M. L. Wis, L. Montanari, M. Milosa and D. Scotti, *J. Org. Chem.*, 1995, **60**, 5446.

11 P. Uznanski, C. Amiens, B. Donnadieu, Y. Coppel and B. Chaudret, *New J. Chem.*, 2001, **25**, 1486.

12 E. Gachard, H. Remita, J. Khatouri, B. Keita, L. Nadjo and J. Belloni, *New J. Chem.*, 1998, **22**, 1257.

13 A. Reiser, L. J. Leyshon, D. Saunders, M. V. Mijovic, A. Bright and J. Bogie, *J. Am. Chem. Soc.*, 1972, **94**, 2414.

14 U. Kreibig and M. Vollmer, *Optical Properties of Metal Clusters*, Springer–Verlag, Berlin and Heidelberg, Germany, 1995.

15 J. Aubard, in *Organic Photochromic and Thermochromic Compounds*, ed. J. C. Crano and R. J. Guglielmetti, Kluwer Academic/Plenum Publishers, New York, 1999, vol. 2, ch. 8.

16 (*a*) N. Chandrasekharan, P. V. Kamat, J. Hu and G. Jones II, *J. Phys. Chem. B*, 2000, **104**, 11 103.(*b*) L. Jeunieau, V. Alin and J. B. Nagy, *Langmuir*, 2000, **16**, 597.

17 N. Felidj, L. J. Pantigny and J. Aubard, *New J. Chem.*, 1998, **22**, 725.